International Journal of Modern Physics B
Vol. 27, No. 18 (2013) 1350069 (13 pages)

DOI: 10.1142/S0217979213500690

World Scientific
www.worldscientific.com

DENSITY FUNCTIONAL CALCULATIONS ON SPECTRUM AND ELECTRONIC PROPERTIES OF W_NCO (N = 1 ∼ 6) CLUSTERS

XIURONG ZHANG*, YANGYANG WANG†, FUXING ZHANG† and AIHUA YUAN‡

*School of Mathematics and Physics,
Jiangsu University of Science and Technology,
Zhenjiang, Jiangsu 212003, P. R. China
†School of Materials Science and Engineering,
Jiangsu University of Science and Technology,
Zhenjiang, Jiangsu 212003, P. R. China
‡School of Biology and Chemical Engineering,
Jiangsu University of Science and Technology,
Zhenjiang, Jiangsu 212003, P. R. China
*zh4403701@126.com

Received 11 January 2013
Revised 23 February 2013
Accepted 4 March 2013
Published 1 July 2013

The spectrum and electronic properties of W_nCO ($n = 1 \sim 6$) clusters have been studied by using density functional theory (DFT) at the B3LYP/LANL2DZ level. It is found that the vibrational frequencies of the strongest infrared intensity are in a range of 1674.3–1846.4 cm^{-1}. For each cluster, the vibration modes at the strongest peak are both IR and Raman active, and be assigned to CO stretching modes. The polarizability analyses indicate that the mean dipole polarizabilities increase monotonically with the increase of cluster size, except W_6CO cluster. In addition, the ionization energies and electronegativities analyses manifest that the W_2CO cluster has well attracted electronic ability; W_6CO cluster is the easiest to lose electrons in all W_nCO clusters.

Keywords: W_nCO ($n = 1 \sim 6$) clusters; spectrum analysis; electronic properties.

PACS numbers: 36.40.Mr, 36.40.Cg, 31.15.E-

1. Introduction

In the past few years, gas molecules adsorbed on transition metal clusters has been widely investigated owing to their unique physical and chemical properties,[1–10] such as extreme hardness, high melting point, chemical inertness, interesting catalytic behavior, etc. Carbon monoxide is one of the most important gases which participate in catalytic processes in heterogeneous phase. Adsorption of carbon monoxide on metal and metalloid surfaces is important, especially for transition metals have been

investigated from many aspects. For example, the interaction of one CO molecule with partial transition metal clusters in geometries and electronic properties by density functional theory (DFT) have been systemically studied by Tian *et al.*[11–14] Several studies concerning the energetic[15,16] and infrared (IR) characteristics[17,18] of CO adsorption on transition metal surfaces have appeared in the articles, even the adsorption of CO on transition metal doped nanotube has been concerned.[19]

It is well known that tungsten metal is one of the important catalysts for the removal of carbon monoxide from auto exhaust gases. Thus, several experiments and theories[20] have been done to comprehend the interaction about CO molecule with tungsten clusters. It was found that adsorption of CO, O_2 on W_n clusters ($n < 10$) have low reactivity and low dependence on cluster size. By pulsed fast flow reactor techniques, the CO reactivity of W_1–W_7 was found to exhibit an essentially monotonic increase with cluster size.[21] Based on the IR spectrum experiments and DFT calculations, Lyon[18] reported that only for smaller W_n clusters with $n = 5 \sim 9, 11$ attributable to C–O stretch vibrations are detectable. For larger clusters there are no noticeable absorption bands observed. Hence, tungsten apparently shows size dependant nondissociative bonding of carbon monoxide on the clusters. Ishikawa *et al.*[22] studied $M(CO)_n$ (M = Cr, Mo, W; $n = 3 \sim 6$) in the gas phase, showed that C and O could well reproduce the absorption frequency and the symmetry characteristic vibrational patterns of CO coordinated in $M(CO)_n$. The results suggest that $M(CO)_{n-1}$ keeps its parent skeleton in $M(CO)_{n-1}$–CO dissociation process.

However, there has been no theoretical study on IR vibration spectrum and static polarizability of the W_nCO ($n = 1 \sim 6$) clusters till now. Recently, the structural, adsorption and electronic properties of one single CO molecule adsorbed on W_n ($n = 1 \sim 6$) clusters have been studied by our group.[23] As an extension work, we perform a comprehensive study on the IR vibration spectrum, static polarizability and thermodynamical property of the W_nCO ($n = 1 \sim 6$) clusters, which could furnish a better understanding in the interaction between CO molecule and tungsten atoms, and could find new functional materials.

2. Computational Methods

In this paper, all calculations for W_nCO ($n = 1 \sim 6$) clusters were performed with the Becke's three parameters hybrid functional (B3LYP) method and the basis set LANL2DZ in the GAUSSIAN 03 program. In order to test the quality of computational methods which we used, we calculated some properties of W_n clusters, CO molecule and WCO cluster. For W_n clusters, the most stable isomers and their optimized geometrical parameter, EA, and dissociation energy (adiabatic and vertical dissociation energies) by using B3LYP/LANL2DZ functional have been reported in our previous works,[24,25] and all in good agreement with available experimental values.[26,27] For a free CO molecule, the bond length 0.116 nm and bond energy 10.98 eV are in accordance with the corresponding experimental values (0.1128 nm and 11.24 eV)[28] and 0.113 nm, 11.02 eV with the 6-311+G(3df)

basis set method. As for WCO cluster, through comparing the B3LYP/LANL2DZ/6-311+G(3df) method (LANL2DZ basis set for W atom, 6-311+G(3df) for CO atoms) and the B3LYP/LANL2DZ method, we could find that they have the same calculated results (bond length about 0.191 nm and spin multiplicity about 5). This test indicates that the B3LYP/LANL2DZ method is reliable and sufficient to the system. Furthermore, we also use Multwifn and Gaussian-View softwares to show the graphics of vibration spectrums and static polarizabilities for W_nCO ($n = 1 \sim 6$) clusters.

3. Results and Discussion

3.1. *Geometrical structure*

One of the most important things in studying clusters is to determine the geometry of the ground states. In order to locate the global minimum and avoiding trapping in the local minima, the initial configurations are obtained by optimizing independent geometries and referring to previous results.[8,26–28] During choosing initial configurations of CO–W_n complexes, the low-lying isomers of bare W clusters were considered as the reactants of CO at various possible adsorption sites, including the atop, bridge and hollow sites. Then the adsorption structures are optimized without any symmetry constraints. Finally, the configuration with the lowest energy is taken as the ground-state structure. The ground-state structures of W_n ($n = 2 \sim 6$) and W_nCO ($n = 1 \sim 6$) clusters[23] are shown in Fig. 1. The blue ball is considered as tungsten atom; the red one represents oxygen atom and the gray ball represents carbon atom. The ground state structures of W_n ($n = 2 \sim 6$) clusters are presented for comparison.

As shown in Fig. 1, comparing with the ground-state structures of bare W_n clusters,[29] the structures of W_nCO ($n = 1 \sim 6$) clusters keep the frame of the corresponding W_n clusters unchanged, except W_4CO cluster. The ground state structures of W_nCO ($n = 4 \sim 6$) clusters are trigonal bipyramid structure, quadrangle and triangular prism structure. With the increase of cluster size, the structural growth model of the W_nCO ($n = 1 \sim 6$) clusters transforms from double-dimensional (2D) to three-dimensional (3D). We also find that most of molecular adsorption states about CO on W_n clusters are end-on type geometries; the bridge site adsorption type geometry plays a supplementary role. The interaction of CO on W_n clusters is a nondissociative adsorption; this is in accordance with the previous experimental values.[21]

3.2. *Vibrational frequencies and spectrum analysis*

The vibrational frequency information about small molecule absorbed on the clusters can usually be used to evaluate the catalytic ability. The vibrational frequency of the strongest IR intensity (^{b}Freq) and the lowest-vibrational frequency (^{a}Freq) about W_nCO ($n = 1 \sim 6$) clusters are listed in Table 1, the vibrational modes are

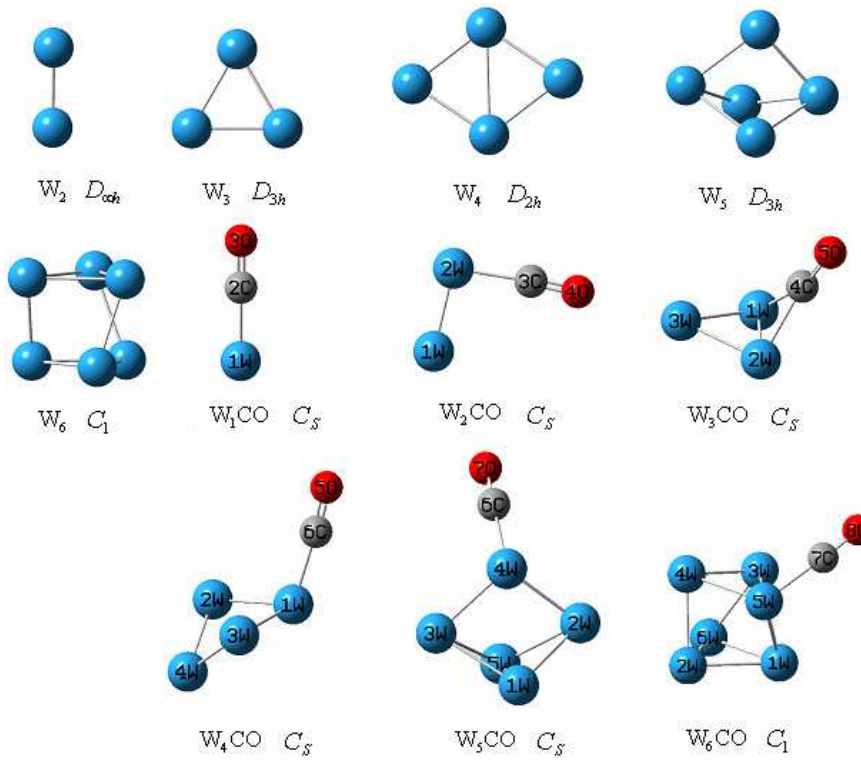

Fig. 1. Ground state structures of W_n $(n = 2 - 6)$ and W_nCO $(n = 1 - 6)$ clusters (obtained in Ref. 23).

Table 1. Vibration frequencies of W_nCO $(n = 1 \sim 6)$ clusters.

Cluster	W_1CO (C_S)	W_2CO (C_S)	W_3CO (C_S)	W_4CO (C_S)	W_5CO (C_S)	W_6CO (C_1)
[a]Freq/(cm^{-1})	374.1 (a')	75.1 (a')	74.2 (a')	56.3 (a')	36.9 (a'')	23.8 (a)
[b]Freq/cm^{-1})	1785.3 (a')	1841.6 (a')	1674.3 (a')	1846.4 (a')	1841.9 (a')	1772.4 (a)

listed in the brackets. The results of vibrational frequency suggest that redshifts of adsorption band occur under the interaction of W atoms. The lowest-vibration frequencies are in a range of 23.8–374.1 cm^{-1}, and all datas are positive numbers. In other words, all the ground state structures of W_nCO $(n = 1 \sim 6)$ clusters are stable and have no transition points. While the vibrational frequencies of the strongest IR intensity varies from 1674.3 to 1846.4 cm^{-1}, and they can show position of the strongest absorption peak in IR spectrum. Whether a mode is IR active or Raman active can be determined by the symmetry. For clusters with C_S symmetry, a' and

a'' modes are both IR and Raman active; for clusters with C_1 symmetry, (a) mode is both IR and Raman active. Generally speaking, our values of frequencies presented here are capable for the following vibrational spectroscopy.

In order to determine the structure of a cluster, no matter by diffraction, electronic or vibrational spectroscopy, comparison of the experimentally obtained spectra with simulated spectra is necessary. In this work, we use B3LYP/LANL2DZ method, calculated the IR spectra and Raman spectra for W_nCO $(n = 1 \sim 6)$ clusters. And, the results are shown in Fig. 2.

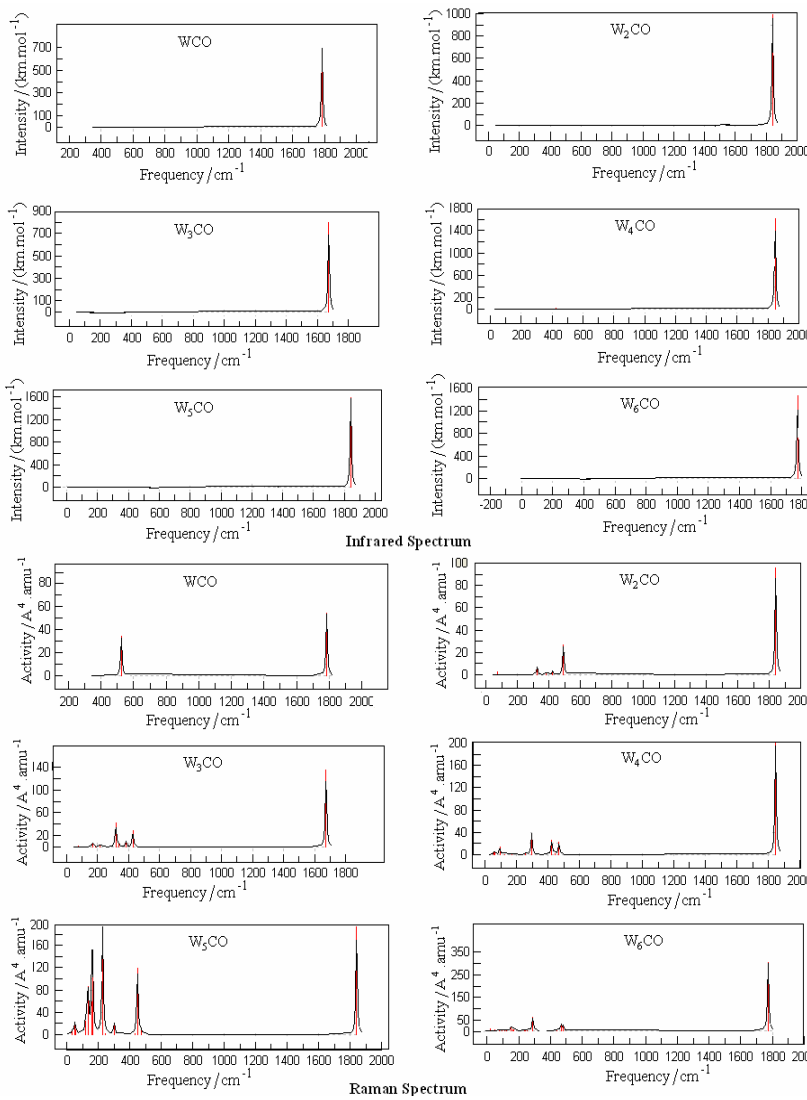

Fig. 2. Calculated IR spectra and Raman spectra of W_nCO $(n = 1 \sim 6)$ clusters.

For W_1CO cluster, the strong peak at 1785.3 cm^{-1} is assigned to the symmetric CO stretching mode with C_S symmetry. The intensity of IR spectrum is 690.1 km.mol^{-1} and 53.8 $A^4 \cdot amu^{-1}$ in the activity of Raman spectrum in this peak, respectively. The other peak observed at 524.7 cm^{-1} in the Raman spectrum having no IR spectrum is assigned to the symmetric W–CO stretching mode. Besides, the W_1CO cluster has the lowest intensity and activity; we have proved it according to the adsorption energy of W_1CO cluster.[23]

For W_2CO cluster, the strong peak at 1841.6 cm^{-1} is assigned to the symmetric CO stretching mode in C_S symmetry. And the intensity of IR spectrum is 995.3 $km \cdot mol^{-1}$ and 95.3 $A^4 \cdot amu^{-1}$ in the activity of Raman spectrum in this peak. The intensities of IR spectrum in other peaks are almost 0 $km \cdot mol^{-1}$. Furthermore, the vibrational frequency at 492.8 cm^{-1} in the Raman spectrum is assigned to a W_2 out-of-plane wagging coupled with CO bend vibration modes with lesser contribution, this result indicates that W–C bonds are very important for the vibration of W_2CO cluster.

The IR spectrum of W_3CO cluster also has one obvious strong peak, which at 1674.3 cm^{-1} with the intensity of IR spectrum is 800.3 $km \cdot mol^{-1}$, which vibration mode is CO stretching mode, the depolarization ratio (D-P) is 0.343, so it has low symmetry. The Raman spectrum of cluster has three obvious peaks, the strongest peak at 1674.3 cm^{-1} is also assigned to CO stretching mode with the activity at 135.4 $A^4 \cdot amu^{-1}$. Both peaks observed at 317.0 cm^{-1} and 426.8 cm^{-1} are assigned to the mixture CO torsion and puckering of W_3 atom modes.

For W_4CO cluster, the peak at 1846.4 cm^{-1} is assigned to W_4 atoms deformation coupled with a CO stretching mode, the corresponding theoretical values are 1604.4 $km \cdot mol^{-1}$ in the intensity of IR spectrum and 199.5 $A^4.amu^{-1}$ in the activity of Raman spectrum. And the peak in the IR spectrum is the strongest one in all W_nCO clusters, so the W_4CO cluster has the largest vibrational mode with C_S symmetry. The two weak peaks in the Raman spectrum were observed at 297.2 cm^{-1} and 424.8 cm^{-1}. The former one's vibration mode is assigned to the asymmetric W atom stretching coupled with CO bend mode, the depolarization ratio is 0.015 with high symmetric vibration mode; the later one's vibration mode is assigned to CO out-of-plane wagging.

For W_5CO cluster, the strongest peak at 1841.9 cm^{-1} is assigned to CO stretching mode with the C_S symmetry, the intensity of IR spectrum is 1598.9 $km \cdot mol^{-1}$ and 193.2 $A^4 \cdot amu^{-1}$ in the activity of Raman spectrum at this peak. Lyon *et al.*[18] have reported that broad bands appear in the spectrum in the 1700–1950 cm^{-1} range by IR vibrational spectra. There are lots of peaks in the Raman spectrum at 0–400 cm^{-1} assigned to mixed W_5 atoms sym stretching and CO asymmetric streching modes, and the activity at $192 \sim 20$ $A^4 \cdot amu^{-1}$. As shown in Fig. 2, the W_5CO cluster in the Raman spectrum has the most strong peaks, because most of the depolarization ratio is 0.750 with high asymmetric vibration mode; on the other hand, W_5CO cluster is the most stable cluster and the length of W–C bond is the shortest among the W_nCO ($n = 1 - 6$) clusters.[23]

For W_6CO cluster, the peak at 1772.4 cm^{-1} is assigned to CO stretching mode with the C_1 symmetry, the intensity of IR spectrum is 1470.6 $km \cdot mol^{-1}$ and 300.6 $A^4 \cdot amu^{-1}$ in the activity of Raman spectrum at this peak. In fact, the W_6CO cluster has the largest activity of the Raman spectrum in W_nCO ($n = 1 - 6$) clusters. However, the weak peak in the Raman spectrum at 288.9 cm^{-1} is assigned to a symmetric streching of W_6 atoms, and the activity is 57.9 $A^4 \cdot amu^{-1}$, it's much lower than the strong peak.

From the vibrational frequencies of W_nCO ($n = 1 \sim 6$) clusters, the vibrational frequencies of the strongest IR intensity are in a range of 1674.3–1846.4 cm^{-1}, similar to those of Ru–CO, Au–CO clusters.[14] For each cluster, the vibration modes at the strongest peak are both IR and Raman active, and be assigned to CO stretching modes. This is mainly caused by two aspects: on the one hand, the strong interaction between W and C atom; on the other hand, CO atoms are the major carriers of negative electron. When the vibrational frequencies wavenumber are low, the vibration mode of cluster is assigned to the W atom stretching coupled with CO stretching.

From the spectrum of W_nCO ($n = 1 \sim 6$) clusters, the IR spectrum graphics of clusters which we studied are similar to each other, this may be caused by the adsorption of the CO molecule. The intensity of IR spectrum is about between 0 $km \cdot mol^{-1}$ and 1605 $km \cdot mol^{-1}$, and the intensity IR spectrum of W_4CO cluster is the strongest than any other W_nCO ($n = 1 \sim 6, n \neq 4$) clusters. On the other hand, the Raman spectrum graphics of the W_nCO ($n = 1 \sim 6$) clusters are different to each other. We can see the activity is in range of 0–300.6 $A^4 \cdot amu^{-1}$. In general, the W_6CO cluster has the largest activity (300.6 $A^4 \cdot amu^{-1}$) of the Raman spectrum in W_nCO ($n = 1 - 6$) clusters, which indicates that the polarizability changed heavily, we will discuss it at below.

3.3. *Polarizability*

In the development of photonic materials, it is important to understand the optical response properties of the materials, specifically the static polarizabilities at the molecular levels.[24] However, there did not present any assignments of the polarizabilities for W_nCO clusters. Here, the polarizability the mean dipole polarizability ($\langle\alpha\rangle$), the mean polarizability per atom ($\langle\bar{\alpha}\rangle$) and the polarizability anisotropy ($\Delta\alpha$) are calculated by using the B3LYP/LANL2DZ method and displayed in Table 2 Furthermore, the mean dipole polarizability ($\langle\alpha\rangle$) and the polarizability anisotropy ($\Delta\alpha$) are defined as in the following formulas[30]:

$$\langle\alpha\rangle = \frac{1}{3}(\alpha_{xx} + \alpha_{yy} + \alpha_{zz})\,, \tag{1}$$

$$\Delta\alpha = \left[\frac{(\alpha_{xx} - \alpha_{yy})^2 + (\alpha_{yy} - \alpha_{zz})^2 + (\alpha_{zz} - \alpha_{xx})^2 + 6(\alpha_{xy}^2 + \alpha_{xz}^2 + \alpha_{zy}^2)}{2}\right]^{\frac{1}{2}}. \tag{2}$$

Table 2. Calculated polarizability of W_nCO ($n = 1 \sim 6$) clusters.

Cluster	Polarizability/a.u								
	α_{XX}	α_{XY}	α_{XZ}	α_{YY}	α_{YZ}	α_{ZZ}	$\langle\alpha\rangle$	$\langle\hat{\alpha}\rangle$	$\Delta\alpha$
W_1CO	73.684	0.000	0.000	73.684	0.000	88.995	78.788	26.263	15.311
W_2CO	137.469	14.549	0.000	129.235	0.000	89.938	118.881	29.720	50.702
W_3CO	153.193	17.244	0.002	174.711	0.000	163.725	163.876	32.775	35.228
W_4CO	158.504	4.389	0.002	259.882	0.000	209.219	209.202	34.867	88.120
W_5CO	266.562	−3.117	0.000	331.971	0.000	311.808	303.447	43.350	58.268
W_6CO	328.130	3.945	−6.232	265.558	−3.740	254.223	282.637	35.330	70.414

As Table 2 shows, we find that the α_{XX}, α_{YY} and α_{ZZ} are the major components for the values of polarizabilities in each cluster. However, in other Cartesian components, the values of polarizability are very small. For W_6CO cluster has large value of polarizability, so the Raman spectrum activity is strong. The value of $\langle\alpha\rangle$ increases monotonically going from W_1CO to W_5CO; however, for W_6CO, the value of $\langle\alpha\rangle$ abruptly descend. Because the geometrical configuration has an effect on the mean dipole polarizability for W_nCO ($n = 1 \sim 6$) clusters. According to the Fig. 1, for W_1CO-W_5CO clusters, the C_S symmetry can be found in their ground state structures, however, the W_6CO is C_1 symmetry. For example, the W_5CO cluster in C_S symmetry has larger $\langle\alpha\rangle$ value than any other clusters, so the W–CO bonding interaction of W_5CO cluster is the strongest in all W_nCO ($n = 1 \sim 6$) clusters.

We also find that the values of mean polarizability per atom present the same trend as mean dipole polarizabilities, W_1CO has the lowest mean polarizability per atom calue in W_nCO ($n = 1 \sim 6$) clusters, which result in a weaker electron delocalization and more compact electronic structure. All the values of $\Delta\alpha$ show the odd–even oscillation behavior, the $\Delta\alpha$ values of the cluster with even W atoms are much larger than those of the clusters with odd W atoms. This result indicates that the response of anisotropy under the external static electric field for the even-size clusters is stronger than the odd-size clusters. Interestingly, this behavior is contrary to Cu_nCO ($n = 1 \sim 9$) clusters.[13] Because the LUMO–HOMO gap for the W_nCO ($n = 1 \sim 6$) clusters[23] is contrary to Cu_nCO ($n = 1 \sim 9$) clusters, showing an opposite electron delocalization between W–CO atoms and Cu–CO atoms.

3.4. *Ionization energies and electronegativities*

The ionization of a molecule by photoionization or by electron impact is governed by the Franck–Condon principles,[31] which suggest that with the increase of ionization energies, the ability to attract electron for a molecule apparently strengthens. Accordingly we calculated the vertical ionization potentials (VIP) and the vertical electron affinities (VEA). These energies are listed in Figs. 3 and 4, respectively.

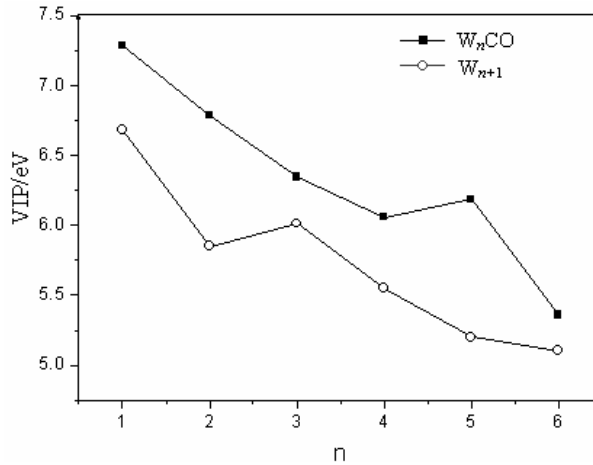

Fig. 3. Values of VIP for W_nCO ($n = 1 \sim 6$) and W_{n+1Ref} clusters.

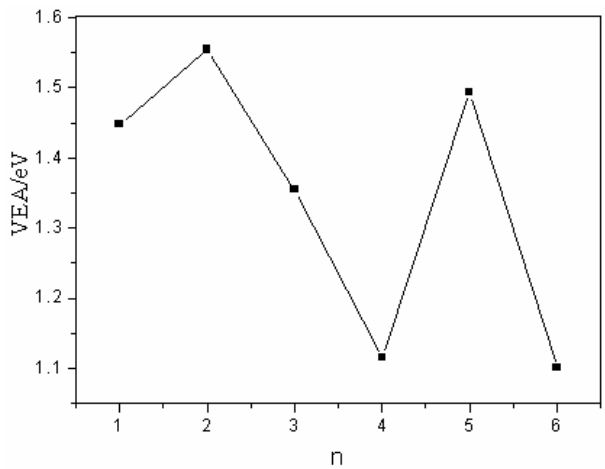

Fig. 4. Calculated values of VEA for W_nCO ($n = 1 \sim 6$) clusters.

They are defined as:

$$E_{\mathrm{VIP}} = E_n^+ - E_n\,, \tag{3}$$

(E_n and E_n^+ both at the geometry of the ground state for W_nCO),

$$E_{\mathrm{VEA}} = E_n - E_n^-\,, \tag{4}$$

(E_n and E_n^- both at the geometry of the ground state for W_nCO^-),

in which E_n is the energy of W_nCO ($n = 1 \sim 6$) clusters and E_n^- is the energy of W_nCO^- cluster.

As shown in Fig. 3, experimental VIP (VIP_{ref}) of W_{n+1} is listed[32] to compare with our results. Our calculated VIP values are greater than the experimental VIP (VIP_{ref}) of W_{n+1}, which suggests that W_nCO clusters are easier to be oxidized than W_{n+1} clusters, so the redox characteristics of W_n are enhanced by adsorbed CO molecule. In addition, the values of VIP for W_nCO clusters decrease as atomic size increases, this means different growth patterns in the geometry structures have different ionizing transition. According to Fig. 4, an oscillation behavior is observed from W_1CO to W_6CO. The W_2CO cluster has the largest value of VEA, while the smallest value of VEA is W_6CO cluster. Which indicates that W_2CO cluster has well attracted electronic ability; however, W_6CO cluster is the easiest to lose electrons in all W_nCO clusters.

The absolute electronegativity (χ) is a good method to measure the ability of molecules attracted electrons. The absolute electronegativity[33] has been defined as:

$$\chi = -(\partial E/\partial N)_\nu \,, \tag{5}$$

where E is the energy and N is the number of electrons in the system considered. In a finite difference approximation using integer values for N, the expressions can be rewritten as[34]:

$$\chi = (\mathrm{VIP} + \mathrm{VEA})/2 \,. \tag{6}$$

Figure 5 displays the χ of W_nCO clusters, the values of χ decrease significantly with the increase in atomic size, except W_5CO cluster. It indicates that the ability to attract electrons of W_nCO ($n = 1 \sim 6, n \neq 5$) clusters becomes lower as the cluster size increases. This may be due to the following reasons: first, the stability of CO on tungsten clusters increase as atomic size increase; second, hybridized orbital has a heavy influence on χ, according to the natural bond orbital (NBO) analysis of

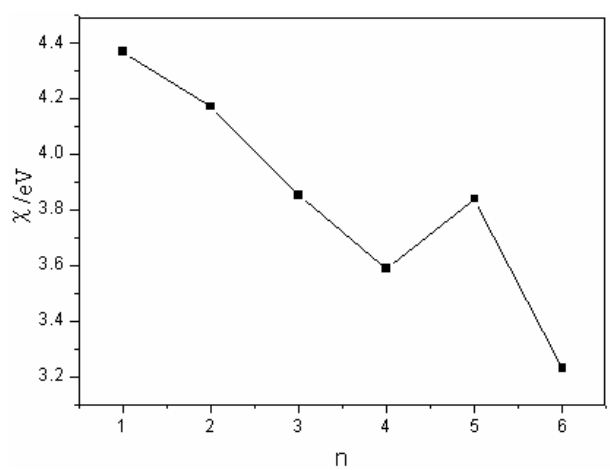

Fig. 5. Calculated values of absolute electronegativity (χ) for W_nCO ($n = 1 \sim 6$) clusters.

Table 3. Thermodynamical properties of W_nCO ($n = 1 \sim 6$) clusters.

	W_1CO	W_2CO	W_3CO	W_4CO	W_5CO	W_6CO
$\Delta H^\theta/(\text{eV})$	−10.723	−14.443	−18.620	−23.151	−28.242	−33.302
$C_V/(\text{Cal}\cdot\text{mol}^{-1}\cdot\text{k}^{-1})$	8.709	13.756	19.700	24.963	30.767	36.322
$S^\theta/(\text{Cal}\cdot\text{mol}^{-1}\cdot\text{k}^{-1})$	56.668	80.932	91.738	104.329	118.935	126.468

W_nCO clusters,[23] the charge transfer among W, C and O atoms are larger than W_n clusters. While the χ value of W_5CO cluster is higher than its neighboring clusters, this is attributed to the ionization energy which is far from the experimental VIP (VIP_{ref}) of W_{n+1}.

3.5. *Thermodynamical properties*

We now discuss the thermodynamical properties of W_nCO ($n = 1 \sim 6$) clusters. Under the condition of the temperature at 298.15 K and the atmospheric pressure at 1.01×10^5 Pa, we calculated the heat capacity at constant volume (C_V), standard entropy (S^θ) and the standard enthalpy of formations (ΔH^θ) of the neutral W_nCO ($n = 1 \sim 6$) clusters by using B3LYP/LANL2DZ method. The results are listed in Table 3. It is well known that if the calculated value of ΔH^θ is negative, the reaction between W atoms and CO molecule is exothermic reaction and the W_nCO ($n = 1 \sim 6$) cluster has strong chemical stability; however, if it is positive, the reaction between W atoms and CO molecule is endothermic reaction and the W_nCO ($n = 1 \sim 6$) cluster has weak chemical stability. The calculated values of ΔH^θ can be obtained from the following formula:

$$\Delta H^\theta = E(W_nCO) - nE(W) - E(C) - E(O)\,, \tag{7}$$

where the $E(*)$ values represent the energies of the ground state structure for W_nCO cluster, free W, O and C atoms, respectively.

As shown in Table 3, the values of ΔH^θ for clusters are all negative numbers, this behavior indicates that the chemical reactions between W atoms and CO molecule are exothermic reactions and the chemical stabilities are good. This behavior is similar to the Holmgren L's results.[20] Furthermore, the results of C_V and S^θ show that the structures of W_nCO cluster increase more stably with an increase in atomic size. The C_V value of per cluster (W_nCO ($n = 2 \sim 6$)) increases 5–6 $\text{cal}\cdot\text{mol}^{-1}\cdot\text{k}^{-1}$, compared with the former one. However, there is no obvious regularity about the increase of S^θ value for per cluster (W_nCO ($n = 2 \sim 6$)).

4. Conclusion

In this paper, based on the ground state structures of W_nCO ($n = 1 \sim 6$) clusters, the spectrum and electronic properties of W_nCO ($n = 1 \sim 6$) clusters have been studied by using DFT at the B3LYP/LANL2DZ level. It is found that the structural growth model of W_nCO clusters transform from 2D to 3D. The vibrational

frequencies and spectrum analysis show that in each cluster, the vibration modes at the strongest peak are both IR and Raman active, and assigned to CO stretching modes. The IR spectrums graphics of clusters which we studied are similar to each other; the Raman spectrum graphics of the W_nCO ($n = 1 \sim 6$) clusters are different to each other.

The polarizability analyses indicate that the α_{XX}, α_{YY} and α_{ZZ} are major components for the values of polarizability in each cluster. The mean dipole polarizabilities increase monotonically with the increase of cluster size, except W_6CO cluster. All the values of polarizability anisotropy show the odd-even oscillation behavior. Both the ionization energies and electronegativities show that the values of VIP for W_nCO clusters decrease as atomic size increases, W_2CO cluster has well attracted electronic ability; W_6CO cluster is the easiest to lose electrons in all W_nCO clusters. According to thermodynamical property analysis, the chemical reactions between W atoms and CO molecule are exothermic reactions and the chemical stabilities are good.

Acknowledgments

This work is partially supported by the National Natural Science Foundation of China (Grant No. 51072072), by the National Natural Science Foundation of Jiangsu Province of China (Grant No. BK2010343).

References

1. M. B. Torres *et al.*, *J. Phys. Chem. A* **115**, 8350 (2011).
2. J. Kukkola *et al.*, *Sens. Actuators. B: Chem.* **153**, 293 (2011).
3. S. Hirabayashi *et al.*, *J. Phys. Chem. A* **116**, 8799 (2012).
4. H. B. Zhou *et al.*, *Prog. Nat. Sci: Mater. Int.* **21**, 240 (2011).
5. G. H. Guvelioglu *et al.*, *Phys. Rev. Lett.* **94**, 026103 (2005).
6. W. S. A. Halim *et al.*, *Appl. Surf. Sci.* **255**, 7547 (2009).
7. Y. Zhao and D. X. Tian, *Comput. Theor. Chem.* **991**, 40 (2012).
8. X. R. Zhang, Z. L. Kang and W. L. Guo, *Chin. Phys. B.* **20**, 103601 (2011).
9. K. P. Prasanth *et al.*, *Int. J. Hydrogen Energy* **35**, 2351 (2010).
10. X. L. Lei, *Chin. Phys. B* **19**, 107103 (2010).
11. F. Y. Tian and J. Shen, *Chin. Phys. B* **20**, 123101 (2011).
12. D. Y. Tang *et al.*, *Acta Chim. Sin.* **70**, 943 (2012), (in Chinese).
13. Z. X. Cao *et al.*, *J. Phys. Chem. B* **106**, 9649 (2002).
14. C. D. Zeinalipour-Yazdi, A. L. Cooksy and A. M. Efstathiou, *Surf. Sci.* **602**, 1858 (2008).
15. F. Amaple *et al.*, *Surf. Sci.* **497**, 139 (2002).
16. Y. Aray *et al.*, *Surf. Sci.* **441**, 344 (1999).
17. A. Fielicke *et al.*, *Surf. Sci.* **603**, 1427 (2009).
18. J. T. Lyon *et al.*, *J. Chem. Phys.* **131**, 184706 (2009).
19. Y. Xie, Y. P. Huo and J. M. Zhang, *Appl. Surf. Sci.* **258**, 6391 (2012).
20. L. Holmgren *et al.*, *Nanostruct. Mater.* **6**, 1009 (1995).
21. D. M. Cox *et al.*, *J. Chem. Phys.* **88**, 111 (1988).
22. Y. Ishikawa and K. Kawakami, *J. Phys. Chem. A* **111**, 9940 (2007).

23. X. R. Zhang *et al.*, *Acta Phys. Sin.* **62**, 053603 (2013) (in Chinese).
24. X. R. Zhang *et al.*, *J. Mol. Struct.: Theochem.* **757**, 113 (2005).
25. X. R. Zhang *et al.*, *J. Mol. Struct.: Theochem.* **867**, 17 (2008).
26. H. Weidele *et al.*, *Chem. Phys. Lett.* **237**, 425 (1995).
27. M. S. Shane, W. S. Adam and D. M. Michael, *J. Chem. Phys.* **116**, 993 (2002).
28. X. Wu *et al.*, *J. Chem. Phys.* **117**, 4010 (2002).
29. W. Yamaguchi and J. Murakami, *Chem. Phys.* **316**, 45 (2005).
30. P. Karamanis, C. Pouchan and G. Maroulis, *Phys. Rev. A* **77**, 013201 (2008).
31. P. Leiva and M. Piris, *J. Mol. Struct.: Theochem.* **719**, 63 (2005).
32. Y. Bai, MS. Thesis, Jilin University, Changchun, China (2008).
33. R. G. Parr *et al.*, *J. Chem. Phys.* **68**, 3801 (1978).
34. X. M. Pan *et al.*, *Synth. Met.* **152**, 325 (2005).